Research on Active Fault Tolerant Control Strategy for Distributed Drive Electric Vehicles Based on Multi-Actuator Failure

Zhigang Zhou, Meizhong Chen, Guanghua Zhang, Wei Shen, Ruili Yang

Abstract—A fault-tolerant control approach, tailored for distributed-drive electric vehicles and centered around optimal torque allocation, is introduced. This method is specifically designed to address single or dual hub motor failures under diverse operational conditions and failure scenarios, including high-speed cornering and accelerated straight-line driving. The proposed method employs a hierarchical architecture, where the upper-level controller utilizes a sliding mode control method to compute the necessary driving torque and adjust the yaw moment in accordance with the driver's inputs and the vehicle's instantaneous operational status. This ensures the vehicle's stability while simultaneously maintaining the slip rate of each wheel within permissible limits. The lower-level controller utilizes the quadratic programming method to allocate the driving torque and the adjusted yaw moment, necessary for maintaining stable vehicle operation, among the four motors. Leveraging the over-actuated nature of distributed-drive electric vehicles, a fault-tolerant control strategy is introduced that considers three pivotal factors: axle load transfer, motor output constraints, and road surface adhesion conditions. This strategy aims to enhance vehicle stability by optimizing the distribution of the remaining tire force. To validate its effectiveness, simulation experiments are conducted across a range of operational scenarios, and the results confirm the utility of the proposed fault-tolerant control method.

Index Terms—Distributed drive electric vehicles, Drive force distribution, Hub motor failure, Handling stability

I. Introduction

Distributed-drive electric vehicles have attracted a lot of attention in electric vehicle research because of its high transmission efficiency, four-wheel independent controllability, and drive system redundancy [1-4].

However, as an over-actuated system, distributed-drive electric vehicles exhibit high system complexity, interconnected subsystems, and numerous actuators, which elevate the risk of subsystem failures [5-8]. Consequently, research into fault-tolerant control for distributed-drive electric vehicles is paramount for enhancing overall vehicle safety and stability.

The term "distributed-drive electric vehicle drive fault-tolerant control" pertains to a control strategy where, in the event of failure of one or more drive motors within the drive-by-wire chassis drive system, the remaining drive motors are effectively redistributed to guarantee the vehicle's driving stability and safety, as described in [9, 10]. The fault-tolerant control strategies for addressing failures in distributed-drive electric vehicles can be categorized into passive fault-tolerant control and active fault-tolerant control, as detailed in [11-13]. Passive fault-tolerant control primarily targets specific types of failures. In the event of a system failure in a vehicle, this approach does not necessitate failure information. Instead, it relies on predefined logic rules to ensure that the rule-based control strategy remains robust against the failure. To ensure system stability and acceptable tracking performance, ZHANG *et al.* [14] investigated the path tracking challenge for an electric vehicle equipped with four drive motors, considering both normal and defective operational conditions. They accomplished this by creating a passive fault-tolerant controller utilizing variable structure control, which incorporated considerations for certain actuator faults and wheel-slip limitations. Within the torque distribution controller, a novel adaptive directional tire force distribution method was introduced to fulfill the control tasks of the upper controller. Additionally, CHEN *et al.* [15] put forward a passive fault-tolerant path-tracking control approach designed to autonomously address steering system faults in distributed-drive electric vehicles. However, the passive fault-tolerant control approach has limitations in accommodating a broader range of fault types in over-actuated systems with numerous potential faults, and optimizing its fault-tolerant effectiveness can be challenging. To ensure the vehicle reaches a safe state and maintains stable driving, active fault-tolerant control can actively mitigate or reduce motor faults, adjust the fault-tolerant controller's parameters in real-time, and adopt a more suitable control strategy tailored to various fault conditions. ZHANG *et al.* [16] tackled the challenge of tracking control in a four-wheel drive electric vehicle amidst actuator faults and disturbances by developing a composite observer. This observer was capable of simultaneously estimating the state of the drive system and the disturbances, reconstructing the fault efficiency factor, and performing self-adaptive tuning of the controller parameters. These capabilities were aimed at

Manuscript received August 16, 2024; revised December 16, 2024. This work was supported by the National Natural Science Foundation of China (51805149); Ningbo Science and Technology Innovation 2025 Major Special Project "Development of Light Electric Vehicle In-wheel Motor and Control System" (2019B10073).

Zhigang Zhou is the professor of Henan University of Science and Technology, Luoyang, 471003, China. (corresponding author, phone: +86 15137976859; e-mail: zhigangzhou@haust.edu.cn).

Meizhong Chen is the postgraduate student of Henan University of Science and Technology, Luoyang, 471003, China. (e-mail: chenmz1099@163.com).

Guanghua Zhang is the postgraduate student of Henan University of Science and Technology, Luoyang, 471003, China. (e-mail: 1592281476@qq.com).

Wei Shen is the postgraduate student of Henan University of Science and Technology, Luoyang, 471003, China. (e-mail: 17633713310@163.com).

Ruili Yang is the postgraduate student of Henan University of Science and Technology, Luoyang, 471003, China. (e-mail: a879453370@163.com).

enhancing tracking performance and robustness. ZHANG *et al.* [17] introduced a fault diagnosis and active fault-tolerant control approach that integrates active front steering (AFS) with direct yaw moment control (DYC). Experimental results demonstrate that this proposed method offers superior active safety while also improving path tracking capability in comparison to other strategies. TANG *et al.* [18] put forward a perturbation-resistant active fault-tolerant control method. This method employs a mismatched nonlinear perturbation observer to estimate perturbations and compensate for modeling errors. Furthermore, they designed an adaptive sliding mode fault-tolerant control strategy, which incorporates the estimated perturbation information into the control rate. This incorporation aims to enhance the overall control performance. MA *et al.* [19] introduced an integrated actuator fault model that encompasses not only efficiency loss faults but also additional bias faults. This model is designed to address actuator faults, time delays, modeling nonlinearities, and external perturbations. The ultimate goal is to enhance the lateral stability and driving active safety of electric vehicles. ZHAO *et al.* [20] tackled the issue of driving stability in the event of single-wheel steering failure. They examined the impact of active rear-wheel steering on vehicle body stability, utilizing a monorail model with additional rear-wheel steering as the steady-state reference model. Based on this, they proposed a hierarchical control method for distributing and reconfiguring tire force. GUO *et al.* [21] developed an active fault-tolerant control system based on the Takagi-Sugeno fuzzy model for the robust lateral control of an autonomous four-wheel independently driven electric vehicle. This system considers the sway effect and actuator failure, specifically focusing on a single hub motor failure. While the studies mentioned above primarily concentrate on fault-tolerant control in the context of a single actuator failure, in distributed-drive electric car over-constraint systems, multiple actuators can fail and are interconnected. Consequently, when multiple actuators fail, fault-tolerant control that only addresses a single actuator may lead to failure due to the coupling effect between the actuators.

In response to the challenges outlined earlier, several researchers have carried out relevant research. ZHANG *et al.* [22] proposed a fault-tolerant control strategy that incorporates multi-method switching. They constructed a control method switching rule by thoroughly analyzing the applicable conditions of various control methods and the impact of application events on the steering system. This strategy not only enhances dynamics and stability in the event of drive motor failure but also significantly improves the efficiency of executing the control strategy. LI *et al.* [23] introduced a fault-tolerant control method that relies on differential steering and drive torque allocation. This method addresses the trajectory tracking problem in a wire-controlled steering system and hub motor when multiple actuators fail simultaneously. They conducted simulation experiments to evaluate the performance of their method in scenarios involving both single actuator failure and simultaneous failure of multiple actuators. The results confirmed the validity of their fault-tolerant control method. ZHOU *et al.* [24] presented a novel diagnostic approach for automobile drive systems that utilizes on-board sensor inputs and the traceless Kalman filtering method. This approach is specifically designed for detecting same-side wheel failure during cornering. Based on the identified fault information, they developed a fault-tolerant control method employing the barrier Lyapunov function. This method ensures vehicle stability even in the event of wheel torque failure by placing constraints on the vehicle's transverse swing rate and lateral velocity. Furthermore, they refined the existing transverse swing fault-tolerant control method by tracking the transverse swing rate and lateral velocity, addressing the inherent instability risks associated with it. LU *et al.* [25] introduced a novel robust fault estimator-based Stochastic Model Predictive Control (SMPC) system specifically designed for distributed drive electric vehicles facing single or double wheel failure issues. This system incorporates a fault estimator to ensure that the lateral motion of the vehicle is controlled and that it tracks the desired longitudinal speed. Additionally, the system accounts for the estimation error of the motor failure degree. Compared to traditional control systems, the improved SMPC system demonstrates a significantly faster response time.

Indeed, the majority of the experiments mentioned previously have focused on regular road conditions, such as steering or straight-line driving, with limited exploration into active fault-tolerant control under extreme operating scenarios like high-speed steering or abrupt acceleration with motor failures. To tackle the challenge of multi-actuator failure in distributed-drive electric vehicles across various operating situations, this research proposes a stability control technique. Specifically, the objective is to introduce a stability management approach that can effectively address multi-actuator failure in distributed drive electric vehicles, ensuring robust performance under a wide range of driving conditions.

The stability control technique includes: (1) instability judgement module: determine the vehicle's instability and select a suitable control mode; (2) Upper controller, which includes a speed following controller, a yaw moment controller, and a slip rate controller, calculates driving torque and adjusts the yaw moment required for the vehicle's stable operation based on the driver's instructions and the current vehicle operation status, while also ensuring that the slip rate of each wheel does not exceed the limit value; (3) Lower level controller: the driving torque and the adjustment of the yaw moment required for the stable operation of the vehicle are allocated to the four motors, and the torque allocation method of optimal allocation is applied to improve the stability of the vehicle; then, CarSim is used to establish the model of the whole vehicle, and Matlab/Simulink is used to establish the model of the stability control strategy and the model of the powertrain, and then joint simulation is carried out to validate the stability control strategy. Finally, the effectiveness of the method is verified by Matlab/Simulink and CarSim joint simulation.

II. Dynamic Modelling of Distributed Drive Electric Vehicles

Vehicle dynamics models are critical in the investigation of post-failure methods for distributed drive vehicle actuators. To this purpose, the vehicle's two-degree-of-freedom reference model, body model, and hub motor model are built

to aid future study. Meanwhile, the hub motor specifications are matched to the electric vehicle's dynamic performance index. Finally, the distributed-drive electric vehicle dynamics model is developed in collaboration with Carsim.

A. Vehicle two-degree-of-freedom reference model

A basic two-degree-of-freedom linear model was employed to study the vehicle's post-failure driving stability [26]. The two-degree-of-freedom reference model is built, as shown in Fig 1, which leads to the determination of the desired yaw rate and mass center side slip angle, as indicated in (1) [27].

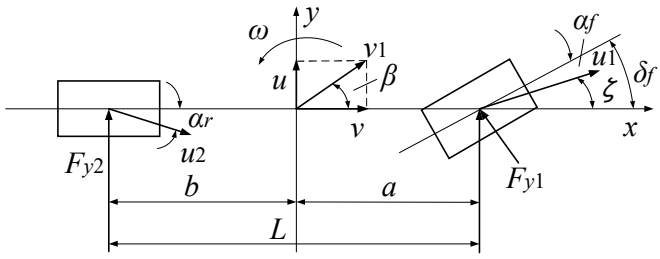

Fig 1. Two degree of freedom reference model

The differential equations for the lateral and transverse motion of the vehicle can be expressed as

$$\begin{cases} \dot{\beta} = \dfrac{k_f + k_r}{mv}\beta + (\dfrac{ak_f - bk_r}{mv^2} - 1)\omega\dfrac{k_f}{mv}\delta_f \\ \dot{\omega} = \dfrac{ak_f - bk_r}{I_z}\beta + \dfrac{a^2k_f + b^2k_r}{I_z v}\omega - \dfrac{ak_f}{I_z}\delta_f \end{cases} \tag{1}$$

where, m represents the vehicle mass, a and b represent the distance between the vehicle's center of mass and the front and rear axles, I_z represents the vehicle's swing moment of inertia, v represents the vehicle's longitudinal speed, ω and β represent the vehicle's yaw rate and side slip angle of the mass center, k_f and k_r represent the stiffness of the front and rear axles' lateral deflection, and F_{y1}, F_{y2} represents the lateral force of the wheels.

The steady-state steering characteristics are used as a characterization of vehicle stability [28]. At this point, $\dot{\omega}$=0, $\dot{\beta}$=0 substituting into (1) yields the expected values of the yaw rate and the side slip angle of mass center, i.e.

Steady-state steering characteristics are used to assess vehicle stability [28,29]. Substituting $\dot{\omega}$=0 and $\dot{\beta}$=0 into (1) produces the predicted values of the yaw rate and side slip angle of the mass center, respectively.

$$\begin{cases} \omega_d = \dfrac{v}{(1+Kv^2)L}\delta_f \\ \beta_d = \dfrac{b + \dfrac{a\cdot mv^2}{k_f\cdot L}}{(1+Kv^2)L}\delta_f \end{cases} \tag{2}$$

$$K = \frac{m}{L^2}(\frac{a}{k_r} - \frac{b}{k_f}) \tag{3}$$

where, K is a stability index that represents the vehicle's stability response parameters.

To avoid an excessive side slip angle of mass center, which causes the vehicle to slip sideways and increases the likelihood of instability, the side slip angle of mass center is assumed to be zero [30]. Thus, the projected yaw rate and side slip angle of mass center are, correspondingly.

$$\begin{cases} \omega_d = \dfrac{v}{(1+kv^2)L}\delta_f \\ \beta_d = 0 \end{cases} \tag{4}$$

B. Body Models

To develop the related drive force distribution management technique and analyze the force situation while driving, the body model illustrated in Fig 2 is built, and the expression between the four-wheel drive force and the additional yaw moment is obtained as

$$\frac{c}{2}(F_{x1} - F_{x2})\cos\delta_f + \frac{c}{2}(F_{x3} - F_{x4}) = M \tag{5}$$

where, F_{x1}, F_{x2} and F_{x3} are the driving forces generated by the four hub motors, M is the additional yaw moment acting on the body, and is the wheelbase.

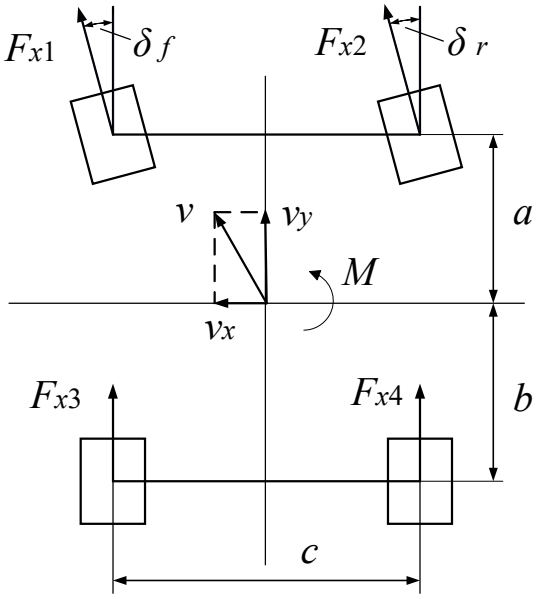

Fig 2. Body rigid body model

Changing the front wheel angle can affect the vehicle's motion state in the direction of the transverse yaw rate, as shown in (1) and (5). The relationship between the yaw rate and the additional front wheel angle δ_f' is

$$\begin{aligned} \dot{\omega} = {} & \frac{ak_f - bk_r}{I_z}\beta + \frac{a^2k_f + b^2k_r}{I_z v}\omega - \frac{ak_f}{I_z}\delta_f \\ & + \frac{M}{I_z} - \frac{ak_f}{I_z}\delta_f' \end{aligned} \tag{6}$$

C. Hub Motor Models

Hub motors are employed as power units in distributed drive electric vehicles, and their properties have a direct impact on the driving performance of these vehicles. To improve the dynamics of hub motors, the vectorial approach is employed to directly adjust motor output torque [31].

A dynamic model can be obtained based on the motor's working principle:

$$J\frac{d\omega_d}{dt} = T_e - T_L \tag{7}$$

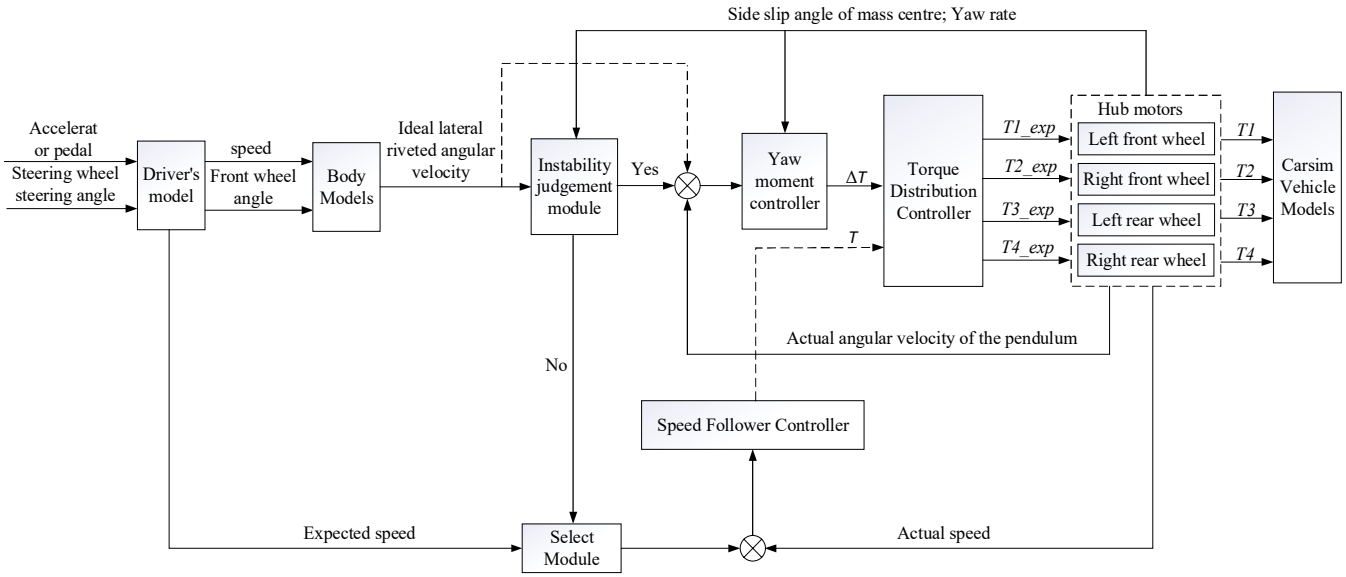

Fig 3. Overall structure of the drive motor failure fault-tolerant control strategy

where, T_e is the load torque, T_L is the driving torque, J is the motor moment of inertia, and ω_d is the angular velocity.

When the drive motor fails, the motor's actual output torque differs from the required torque. To identify the faulty motor from the non-faulty motor, a fault factor is added to express the relationship between the motor output torque and the desired torque:

$$\lambda_i = \frac{T'_{xi}}{T_{xi}} (0 \le \lambda_i < 0) \tag{8}$$

where, λ_i is the failure factor, λ_i=0 indicating a full failure of the hub motor and $0<\lambda_i<1$ indicates a partial failure of the drive motor. T_{xi} and T'_{xi} (i=1-4) indicate the required and output torques of the four hub motors, respectively.

When combined with the hub motor's output capacity, the drive's achievable range can be written as

$$\lambda_i \frac{T_{\min}}{R} \le F_{xi} \le \lambda_i \frac{T_{\max}}{R} \tag{9}$$

where, T_{min} and T_{max} are the minimum and maximum torques, signifying the motor's minimum and maximum output; R is the tire's effective radius respectively.

III. Driving Force Distribution Control Strategy

Control architectures are developed for four-wheel normal hub motor drive force distribution and faulty hub motor drive force distribution, respectively, to ensure the safe and stable operation of distributed-drive electric cars in the event of single-motor or dual-motor failures. First, using the deviation of the traveling speed, the PID controller is designed to determine the total longitudinal force F. This is then combined with the yaw rate ω and the side slip angle of the mass center β. The controller is then designed M_ω and M_β constructed to obtain the additional yaw moment M with the weighting module. Second, at the allocation layer, the objective function and restrictions are employed to create the optimal allocation mathematical model, and the solution is optimized using quadratic programming. Among them, if the drive motor fails and is limited by the motor's output capacity on the same side, preventing the car from continuing on the planned trajectory, cooperative front wheel steering is used to preserve the vehicle's safe and stable driving. The overall control strategy structure diagram is shown in Fig 3.

A. Design of yaw moment controller

The yaw moment controller's objective is to ensure that the side slip angle of the vehicle's mass center changes within a small range while keeping the yaw rate as close to the target value as possible. At the same time, there is a coupling relationship between the two, and it is difficult to create a satisfactory control effect by tracking only the intended yaw rate and the mass center's side slip angle, therefore the control variables must be weighted.

1) M_ω controller design based on yaw rate

When the mass center's side slip angle is minimal, the difference between the actual and target yaw rate values should be kept to a minimum in order for the vehicle to effectively follow the driver's steering demand. In this study, the sliding mode theory is employed to construct the controller, specifying the deviation and the sliding mode surface.

$$s_\omega = c_1 e_\omega \tag{10}$$

Substituting (1) into (8) and calculating it yields

$$\begin{aligned} \dot{s}_\omega &= c_1 \left(\frac{ak_f - bk_r}{I_z} \beta + \frac{a^2 k_f + b^2 k_r}{I_z v} \omega - \frac{ak_f}{I_z} \delta_f - \omega_d \right) + c_1 \frac{M_\omega}{I_z} \\ &= X + c_1 \frac{M_\omega}{I_z} \end{aligned} \tag{11}$$

To approximate the slip mode surface, an exponential convergence rate is used.

$$\dot{s}_\omega = -k_1 \operatorname{sgn}(s) - \varepsilon_1 s_\omega \tag{12}$$

where, ε_1 and k_1 are the exponential convergence rate coefficients, ε_1>0 and k_1>0.

Combining (9) and (10) yields

$$M_\omega = -\frac{I_z}{c_1} \cdot [X + k_1 \operatorname{sgn}(s) + \varepsilon_1 s] \tag{13}$$

2) Controller design based on side slip angle of mass center

When the side slip angle of mass center is too large, the

driver will be unable to manage the vehicle's swing direction movement through the steering wheel, and the vehicle will be unstable or even dangerous to operate. Therefore, the side slip angle of mass center should be reduced.

The phase plane β-$\dot{\beta}$ separates the vehicle's stable and unstable domains [32-34]. To maintain stability, the deviation $e_\beta=\frac{1}{24}\dot{\beta}+\frac{4}{24}\beta$ is determined using phase plane theory. The sliding mode surface is described as

$$s_\beta = c_2 e_\beta \tag{14}$$

where, c_2 is the coefficient of deviation of side slip angle of mass center, $c_2>0$.

Substituting (1) into (12) yields

$$\dot{s}_\beta = Y + (\frac{ak_f - bk_r}{mv^2} - 1)\frac{M_\beta}{I_z} \tag{15}$$

Similarly, the exponential convergence rate coefficients are chosen, i.e.

$$\dot{s}_\beta = -k_2 \operatorname{sgn}(s) - \varepsilon_2 s_\beta \tag{16}$$

where, ε_2 , k_2 are the exponential convergence rate coefficients, and $\varepsilon_2>0$, $k_2>0$.

Meanwhile, the joint (13) and (14) can be obtained as

$$M_\beta = -I_z(Y + k_2 \operatorname{sgn}(s) + \varepsilon_2 s)\cdot(\frac{ak_f - bk_r}{mv^2} - 1)^{-1} \tag{17}$$

3) Stability analysis of sliding mode control

Define the Lyapunov function as

$$V = \frac{1}{2}s^2 \tag{18}$$

Stability analysis of a M_ω controller based on yaw rate:

$$\begin{aligned} \dot{V} &= s_\omega \cdot \dot{s}_\omega \\ &= s_\omega \cdot [-k_1 \operatorname{sgn}(s) - \varepsilon_1 s_\omega] \\ &= -k_1 \cdot |s_\omega| - \varepsilon_1 \cdot s_\omega^2 \end{aligned} \tag{19}$$

Stability analysis of the M_β controller based on the side slip angle of mass center:

$$\begin{aligned} \dot{V} &= s_\beta \cdot \dot{s}_\beta \\ &= s_\omega \cdot [-k_2 \operatorname{sgn}(s) - \varepsilon_2 s_\beta] \\ &= -k_2 \cdot |s_\beta| - \varepsilon_2 \cdot s_\beta^2 \end{aligned} \tag{20}$$

since k_1 and k_2 are bigger than zero, ε_1 and ε_2 are greater than zero, indicating that the system is stable according to the Lyapunov stability condition ($\dot{V}\leq 0$).

4) Weighted design of yaw moment

Before weighting the yaw moment control quantity, the switching function is sgn(s), which has discontinuity characteristics and produces jitter array when switching up and down the sliding mode surface; therefore, the saturation function is chosen to replace the sign function:

$$sat(s) = \begin{cases} 1, s \geq \varphi \\ \dfrac{s}{\varphi}, |s| \leq \varphi \\ -1, s \leq -\varphi \end{cases} \tag{21}$$

The slip mode thickness, denoted by φ, s is represented by s_ω and s_β respectively.

Coupling between yaw rate and side slip angle of the mass center. Thus, this paper combines the relevant phase plane theory to design the weighted control module. When the vehicle is in the stable domain, tracking the yaw rate meets path requirements. When it is between the stable and dangerous domains, the M_β controller intervenes to avoid dangerous control domains. When it is in the dangerous domain, the M_β control domain is used to restore stability first. Let ρ be the weight coefficient of M_ω, where $\rho < 1$.

$$\rho = \begin{cases} 1, \left|\frac{1}{24}\dot{\beta} + \frac{4}{24}\beta\right| \leq 0.8 \\ 1 - \left|\frac{1}{24}\dot{\beta} + \frac{4}{24}\beta\right|, 0.8 \leq \left|\frac{1}{24}\dot{\beta} + \frac{4}{24}\beta\right| \leq 1 \\ 0, \left|\frac{1}{24}\dot{\beta} + \frac{4}{24}\beta\right| \geq 1 \end{cases} \tag{22}$$

Ultimately, an expression for the weighted yaw moment is obtained:

$$M = \rho \cdot M_\omega + (1-\rho)\cdot M_\beta \tag{23}$$

B. Vehicle speed following controller design

Vehicle speed is an important characteristic in vehicle drive control since it characterizes vehicle dynamics and is directly managed by the driver, who constantly wants to be able to track the vehicle speed while driving. As a result, the desired speed can be determined based on the driver's accelerator pedal travel, the total longitudinal force can be calculated based on the actual and desired speeds, and the optimal torque can then be distributed to each actuator in conjunction with the lateral tracking control module.

To simplify the complexity of the vehicle control system and increase its dependability, a PID controller solves and calculates the total longitudinal force using the mathematical expression:

$$F = K_P \cdot e(t) + K_I \int e(t)dt + K_D \frac{de(t)}{dt} \tag{24}$$

where, $e(t)$ is the deviation of the actual speed from the desired speed, i.e., $e(t)=v-v_d$; K_P, K_I, and K_D are the proportional, integral, and differential coefficients in the PID controller, respectively.

C. Drive distribution control

1) Drive force distribution control under normal operation of drive motors

The primary moments of the drive force allocation calculate the total longitudinal force and yaw moment requirement, as well as the optimization target of the control volume given to the four drive motors, while keeping the various limitations in mind. When the vehicle is driving normally, the lateral force created in the tire is one of the primary sources of instability, hence the lateral margin is employed as the optimization objective function:

$$\min J_1 = \sum_{i=1}^{4} \frac{F_{xi}^2 + F_{yi}^2}{(\mu F_{zi})^2} \tag{25}$$

The vehicle faces multi-dimensional condition constraints

$$R_1: \begin{cases} \frac{c}{2}(F_{x1} - F_{x2})\cos\delta_f + \frac{1}{2}(F_{x3} - F_{x4}) = M \\ (F_{x1} - F_{x2})\cos\delta_f + (F_{x3} + F_{x4}) = F \\ \frac{T_{\min}}{R} \leq F_i \leq \frac{T_{\max}}{R} \\ -\sqrt{(\mu F_{zi})^2 - F_{yi}^{\ 2}} \leq F_{xi} \leq \sqrt{(\mu F_{zi})^2 - F_{yi}^{\ 2}} \end{cases} \tag{26}$$

while driving; here, the equation constraints are the yaw moment and longitudinal force demand, and at the same time, constraints such as the drive motor capacity and road surface attachment conditions must be considered, which can be combined to obtain the constraints R_1.

where, u is the tire pavement adhesion coefficient; $F_{zi}(i$=1-4) is the vertical pavement load.

2) Drive distribution control in case of drive motor failure

Since the control allocation under normal drive is solved based on rigid equation constraints, no feasible solution may occur when the drive motor fails or the drive force is saturated [35], therefore, the optimization objective function under drive motor drive is set up to relax the mandatory and constraints of the equation, and transform it into an objective to satisfy the vehicle's transverse stability and dynamics as much as possible; then, the drive motor is taken into consideration capacity constraints, attachment conditions and other inequality constraints, and then achieve the optimal solution of the four-wheel drive force.

Therefore, the mathematical model of optimal drive force allocation under drive motor failure can be expressed as a relation containing the optimization objective function J_2 and constraints R_2:

$$\min J_2 = \left\| \omega(Bu - y) \right\|_2 \tag{27}$$

$$R_2 : \begin{cases} \lambda_i \cdot \dfrac{T_{\min}}{R} \le F_{xi} \le \lambda_i \cdot \dfrac{T_{\max}}{R} \\ -\sqrt{(\mu F_{xi})^2 - F_{yi}^{\ 2}} \le F_{xi} \le \sqrt{(\mu F_{xi})^2 - F_{yi}^{\ 2}} \end{cases} \tag{28}$$

where, ω is the longitudinal force and yaw moment weight coefficient matrix; y and B are the coefficient matrix and state matrix for (26), respectively.

$$y = \begin{bmatrix} F & M \end{bmatrix} \tag{29}$$

$$B = \begin{bmatrix} \cos\delta_f & \cos\delta_f & 1 & 1 \\ \dfrac{c}{2}\cos\delta_f & -\dfrac{c}{2}\cos\delta_f & \dfrac{c}{2} & -\dfrac{c}{2} \end{bmatrix} \tag{30}$$

The control variable is the driving force of the four wheels:

$$u = \begin{bmatrix} F_1 & F_2 & F_3 & F_4 \end{bmatrix}^T \tag{31}$$

3) Cooperative front wheel steering distribution control under drive motor failure

When the drive motor fails, the drive force redistribution causes a rise in the driving force of the wheel on the same side as the failure, especially if the actuator is over-actuated and driven to attain its highest torque output. The motor will burn out in a short period of time, reducing the torque output; and because the drive motor is over-actuated, it cannot generate enough yaw moment solely through drive force distribution, and the wheel will deviate from the expected trajectory; thus, when the drive motor reaches its output limit, it is considered to be controlled by distribution in coordination with front wheel steering.

Let $M_\omega^{'}$=M_ω-$ak_f \cdot \delta_f^{'}$, then we have

$$\dot{\omega} = \frac{ak_f - bk_r}{I_z}\beta + \frac{a^2k_f + b^2k_r}{I_z}\omega - \frac{ak_f}{I_z}\delta_f + \frac{M'_\omega}{I_z} \tag{32}$$

Similarly, the sliding mode function is designed using the exponential convergence rate, and the weighting module is utilized to calculate the additional yaw moment:

$$M' = \rho \cdot M'_\omega + (1-\rho) \cdot M_\beta \tag{33}$$

Similarly, (32) is relaxed to remove the slack constraints and transformed into (34) with the control objectives of transverse stability and dynamics, and integrates the drive motor capacity, front wheel angle additional range, and road surface attachment inequality constraints, allowing for the optimal solution of the four-wheel drive force and front wheel steering angle. The improved goal function $J_2^{'}$ and constraints R_2' of the synergistic front-wheel steering distribution controller under drive motor failure are as follows

$$\min J_2' = \left\| \omega(B'u' - y') \right\|_2 \tag{34}$$

$$R_2' : \begin{cases} \lambda_i \cdot \dfrac{T_{\min}}{R} \le F_{xi} \le \lambda_i \cdot \dfrac{T_{\max}}{R} \\ \delta'_{f\min} \le F_{xi} \le \delta'_{f\max} \\ -\sqrt{(\mu F_{xi})^2 - F_{yi}^{\ 2}} \le F_{xi} \le \sqrt{(\mu F_{xi})^2 - F_{yi}^{\ 2}} \end{cases} \tag{35}$$

where, $y^{'}$ and $B^{'}$ are the coefficient and state matrices for (33), respectively.

$$y' = \begin{bmatrix} F & M' \end{bmatrix} \tag{36}$$

$$B' = \begin{bmatrix} \cos\delta'_f & \cos\delta'_f & 1 & 1 & 0 \\ \dfrac{c}{2}\cos\delta'_f & -\dfrac{c}{2}\cos\delta'_f & \dfrac{c}{2} & -\dfrac{c}{2} & -ak_f \end{bmatrix} \tag{37}$$

The control variables are the drive force of the 4 wheels and the additional steering angle of the front wheels:

$$u' = \begin{bmatrix} F_1 & F_2 & F_3 & F_4 & \delta'_f \end{bmatrix} \tag{38}$$

D. Optimal allocation solving based on quadratic programming

Distributed drive electric vehicle drive allocation methods are fundamentally optimization problems with constraints, and the quadratic programming optimization solution approach is used here, which is well handled and fits the drive allocation application criteria. The quadratic programming-based relationship expression is

$$\begin{cases} \min \dfrac{1}{2} x^T H x + f^T x \\ Ax \le B \\ A_{eq} x \le B_{eq} \\ l_b \le x \le u_b \end{cases} \tag{39}$$

where, H is the real symmetric matrix after the processing of the optimal objective function; f is the vector of primary terms in quadratic programming; A and B are the coefficient matrices and the column vectors at the right end of the inequality constraints, respectively; A_{eq} and B_{eq} are the coefficient matrices and the column vectors at the right end of the equilibrium constraints, respectively; and l_b and u_b are the lower limit and upper limit constraints on the control volume, respectively.

IV. Simulation Verification

To test the effectiveness of the driving force distribution control strategy proposed in this paper, a joint simulation model is created, and simulation analysis is performed using Carsim and Simulink, with Carsim providing the vehicle dynamics model, control strategy, and optimized distribution algorithm implemented in Simulink. Meanwhile, to better compare the simulation effect, the method of distributing the

total driving force to four wheels is defined as average distribution, and the distribution method built using the above strategy is defined as optimized distribution, which is compared to different working conditions to verify the control effect of optimized distribution.

TABLE I
EXPERIMENTAL PARAMETERS

Name	Value	Name	Value
The vehicle mass m /kg	1765	Tread (on tire) c /m	1.48
Vehicle yaw moment of inertia I_z/(kg·m^2)	2700	Front and rear axle Front axle lateral deflection stiffness k_f /(N·rad^{-1})	150000
Distance of the center of mass from the front axle a /m	1.20	Rear axle lateral deflection stiffness k_r /(N·rad^{-1})	150000
Distance of the center of mass from the rear axle b /m	1.40	Maximum motor output torque T /(N·m)	1000

A. Driving simulation analysis of left front wheel failure during cornering driving

When the left front wheel is completely disabled at 4s, the vehicle speed is set to 90km/h, the road adhesion coefficient is 0.85, and a sinusoidal cornering angle with an amplitude of 45° is applied to the steering wheel at 3s with a period of 4s to simulate the cornering driving condition. Fig 4 – Fig 8 illustrate the simulation results of the vehicle reaction without control and with optimum distribution control.

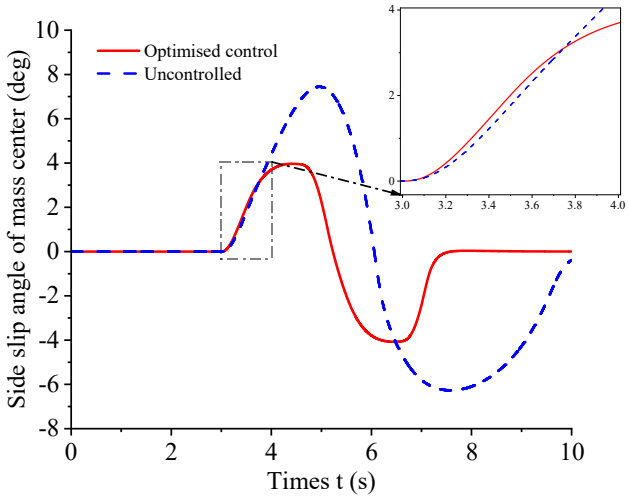

Fig 4. Side slip angle of mass center curve

Fig 4 depicts the curve of the vehicle's side slip angle at the mass center under no control and optimally assigned control. The side slip angle of mass center increases in the third second of steering; in the fourth second, due to the complete failure of the left front wheel, the magnitude of the change of the optimized distribution angle is obviously smaller than that of the curve in the uncontrolled condition; at 7s, when the steering wheel is set to 0, the optimized distribution control of the side slip angle of mass center also returns to normal quickly, making the vehicle more stable.

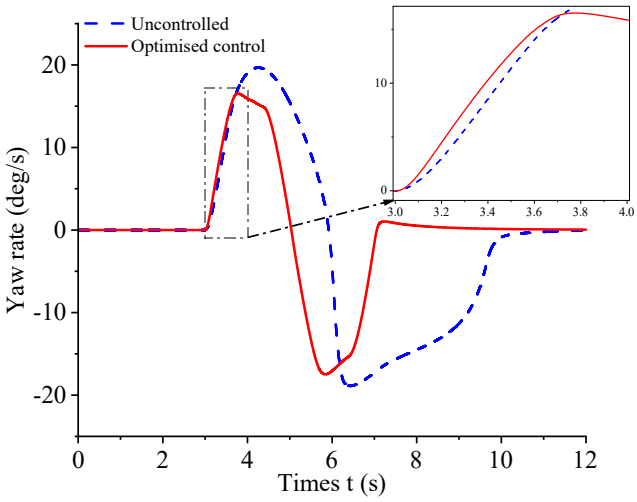

Fig 5. Yaw rate curve

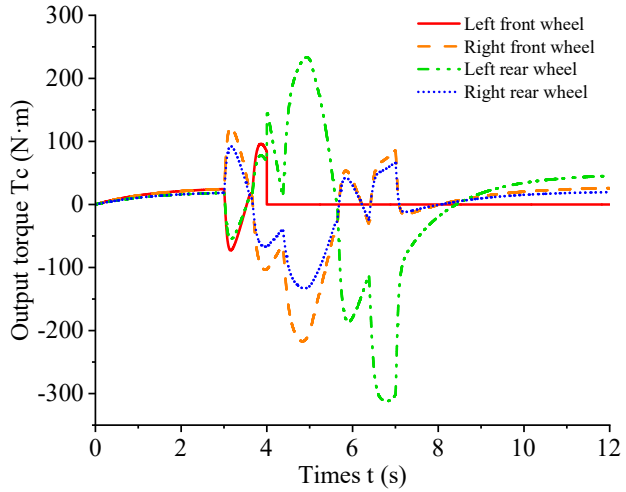

Fig 6. Four-wheel torque variation curve

Fig 5 and Fig 6 show that the failure of the outer motor during the right turn of the vehicle causes the vehicle to understeer, and during the left turn of the vehicle, the faulty motor changes to the inner side, causing the motor to oversteer, and in order to reduce the error of the yaw rate, the drive motors become over-saturated, so the active steering strategy is used to reduce the error value.

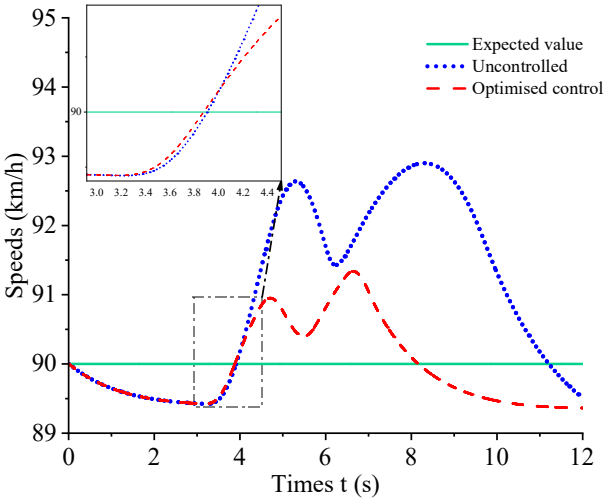

Fig 7. Vehicle speeds change curve

Fig 7 demonstrates that the left front wheel fails entirely at the fourth second under the fault-tolerant controller. This illustrates that the optimized vehicle speed changes are lower and cornering driving is more stable, which ensures the vehicle's safety in the event of a cornering driving failure.

B. Simulation analysis of left front wheel and right rear wheel faults during cornering driving

The vehicle speed is set to 90 km/h, the road adhesion coefficient is 0.85, and a sinusoidal cornering angle with an amplitude of 45° is applied to the steering wheel at 3 s with a period of a fourth of a second to simulate the cornering driving condition. The figures illustrate the simulation results for the vehicle's reaction when there is no control in place, as well as when optimal distribution control is employed.

Fig 8 illustrates the four-wheel drive vehicle in the two-wheel failure conditions of the side slip angle of mass center during the simulation process. It can be observed that the vehicle subsequently assumes a negative value with respect to the right turn, exhibiting a notable reduction in amplitude and failing to achieve the anticipated steering effect, which in turn affects the stability of the vehicle when cornering.

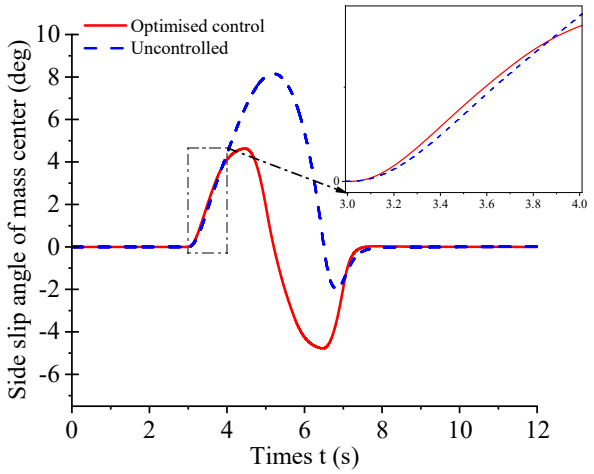

Fig 8. Side slip angle of mass center curve

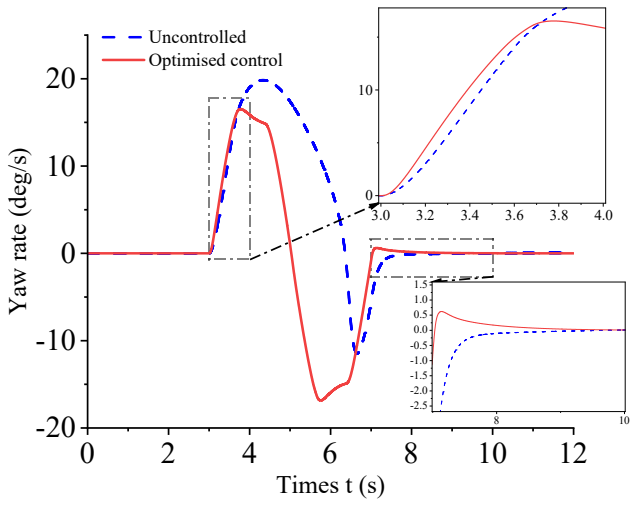

Fig 9. Yaw rate curve

From Fig 9 and Fig 10, it can be seen that in the simulation process, the opposite side of the motor failure after the no control process will produce the transverse swing angular velocity and its instability, resulting in error. By optimizing the allocation method, it can control the left and right side wheel drive torque to achieve the vehicle's lateral tracking ability. At the same time, the center of mass lateral deflection angle remains consistent, considerably improving the vehicle's stability.

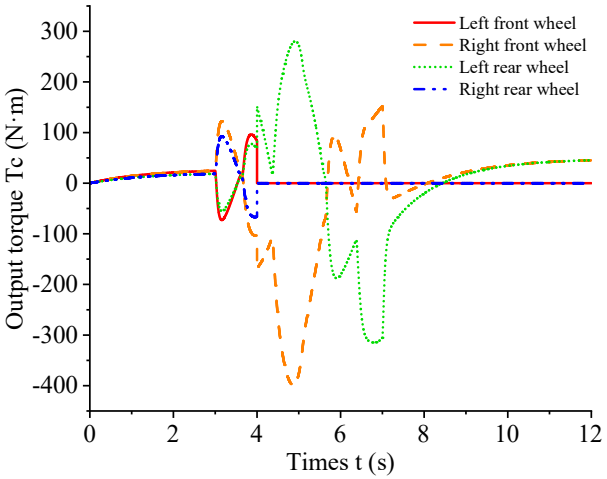

Fig 10. Four-wheel torque variation curve

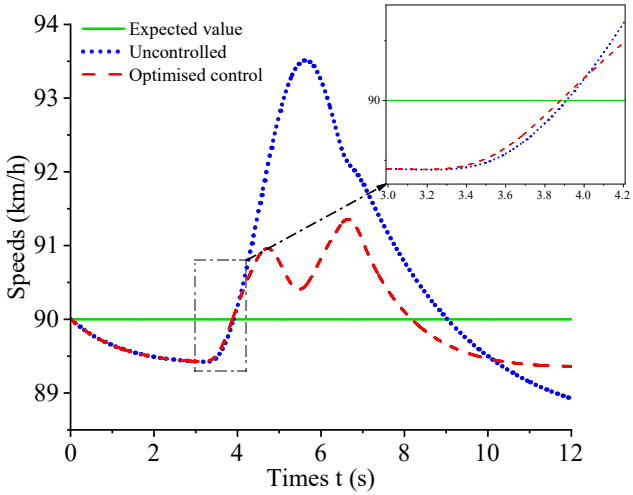

Fig 11. Vehicle speeds change curve

C. Simulation analysis of left front wheel and right rear wheel failure during straight line accelerated driving

When the vehicle is in a state of uninterrupted motion in a straight line, the longitudinal speed is increased from 54km/h to 90km/h. The road surface adhesion coefficient is 0.85, the left front wheel is rendered completely inoperable at 4s, and the right rear wheel is completely disabled at 7s. The figure below depicts the comparative effect of the vehicle's response under the control of the fault-tolerant controller.

Fig 13 and Fig 14 illustrate that the motor failure 4s and 7s results in a deviation from the desired trajectory. Additionally, the motor on the same side of the failure increases the torque output, which in turn causes an increase in the yaw rate and side angle. The side angle of mass center slip angle rapidly approaches the desired value due to the setting of the slip mould thickness at 0.1. The yaw rate error values remain within the limitations of the transverse pendulum moment equation, enabling the vehicle to maintain the target speed with minimal change in dynamics.

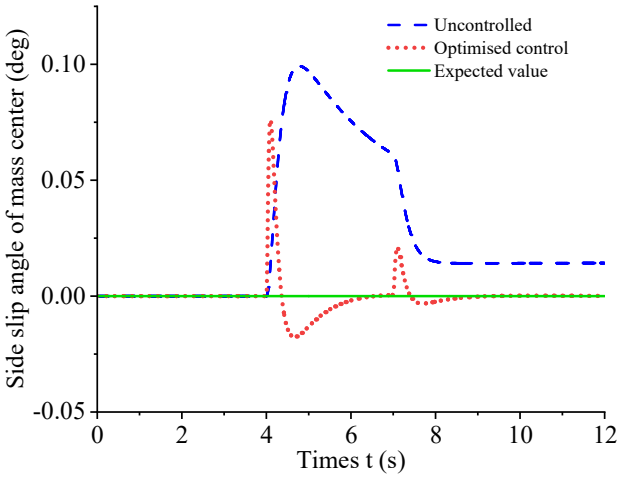

Fig 12. Side slip angle of mass center curve

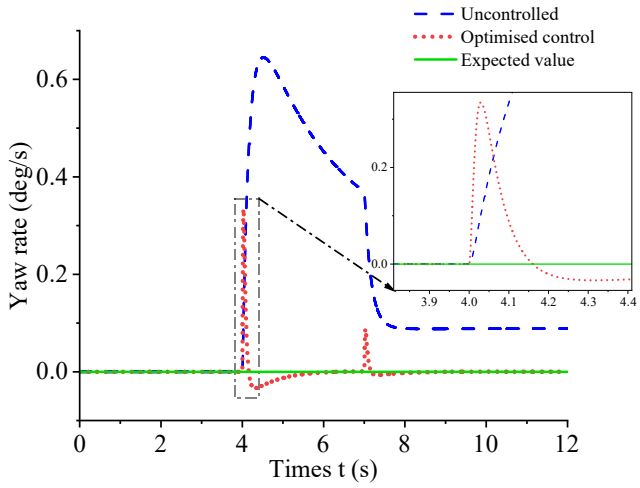

Fig 13. Yaw rate curve

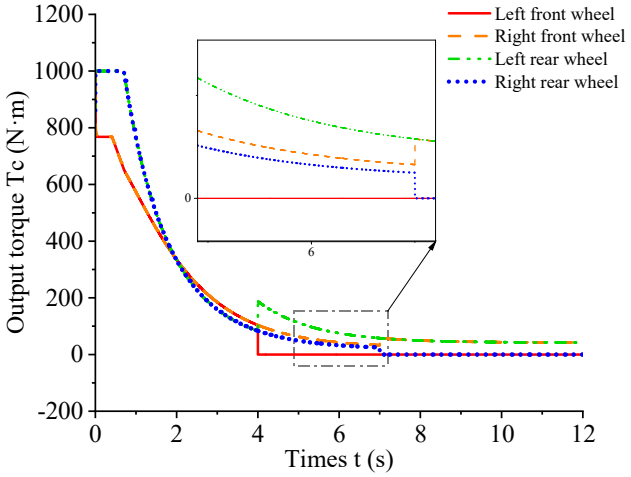

Fig 14. Four-wheel torque variation curve

Fig 15 depicts the change curve of vehicle speed under this circumstance, demonstrating that the vehicle speed is closer to the target value after fault-tolerant control, and the vehicle travels more steadily. Because this study does not compromise dynamics in order to improve safety and stability, but instead use coordinated control to boost lateral force and swing moment, the vehicle speeds are all around the intended level. The simulation results suggest that this distribution approach can assure the vehicle's safety, stability, and dynamic performance.

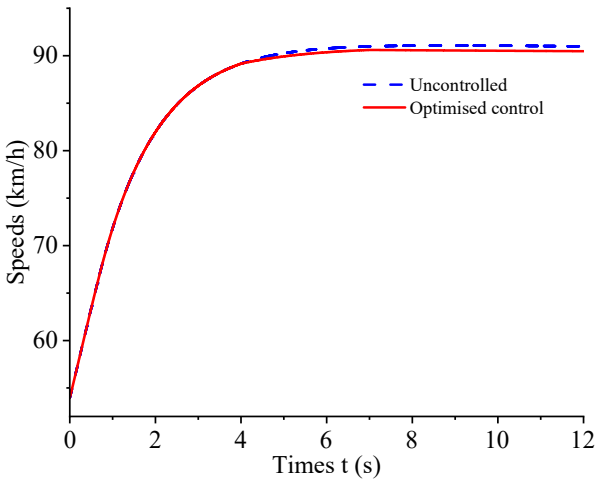

Fig 15. Vehicle speeds change curve

V. Conclusion

(1) An upper-level controller, which incorporates a yaw moment controller and a vehicle speed following controller, is designed to calculate the driving torque required for stable vehicle driving and adjust the yaw moment output to the lower-level controller. Additionally, a lower-level torque distribution controller is included, which considers the hub motor's failure-tolerant control for torque redistribution.

(2) This paper presents a torque distribution approach that takes into account axle load transfer, motor output limitation and road surface adhesion conditions. The results demonstrate that effective fault-tolerant control may be executed independently of single or dual wheel failure in high-speed cornering or dual-wheel failure in accelerating in a straight line, thus enabling reasonable torque distribution following hub motor failure under the constrained operational conditions. The system maintains a favorable side slip angle of mass center and yaw rate, thus ensuring the stability of the vehicle. Conversely, the system is designed to maintain the vehicle's speed following the loss of drive motors, thereby ensuring the vehicle's dynamic stability.

(3) Simulation and verification testing were conducted under high-speed cornering and accelerated straight-line driving scenarios using the Matlab/Simulink and CarSim joint simulation platforms. The proposed fault-tolerant control methodology has been shown to enhance the vehicle's stability and safety in the event of failure under high operating conditions, in both single-hub and dual-hub motor failure scenarios.

REFERENCES

[1] X. Fan and H. Li, "Review on electronic differential system for electric vehicles," *Int. J. Heavy Veh. Syst.*, vol. 31, no. 3, 2024.

[2] A. Karki, S. Phuyal, D. Tuladhar, S. Basnet, and B. Shrestha, "Status of Pure Electric Vehicle Power Train Technology and Future Prospects," *ASI*, vol. 3, no. 3, p. 35, Aug. 2020.

[3] K. Xu, Y. Luo,Y. Yang and G. Xu, "Review on state perception and control for distributed drive electric vehicles," *Journal of Mechanical Engineering*, vol. 55, no. 22, pp. 60–79, 2019.

[4] C. Feng, N. Ding, Y. HE, G. Xu and F. Gao, "Design of a comprehensive chassis control system for a distributed drive electric vehicle," Automotive Engineering, vol. 37, no. 2, pp. 207–213, 2015.

[5] M. Dalboni *et al.*, "Nonlinear Model Predictive Control for Integrated Energy-Efficient Torque-Vectoring and Anti-Roll Moment Distribution," *IEEE/ASME Trans. Mechatron.*, vol. 26, no. 3, pp. 1212–1224, Jun. 2021.

[6] Y. Zou, N. Guo, X. Zhang, X. Yin, and L. Zhou, " Review of Torque Allocation Control for Distributed-drive Electric Vehicles," *China Journal of Highway and Transport*, vol. 34, no. 9, pp. 1–25, 2021.

[7] X. Zhao, Z. Wang, J. MA, Q. Yu, and Z. Zheng, "Review of chassis integrated control technology for distributed drive electric vehicles," *China Journal of Highway and Transport*, vol. 36, no. 4, pp. 221–248, 2023.

[8] Z. Zhou, X. Ding, Z. Shi, X. Yin, and X. Meng, "In-wheel Motor Electric Vehicle Based on Fuzzy Neural Network Yaw Stability Optimization Control," *Engineering Letters*, vol. 31, no. 4, pp1717-1723, 2023.

[9] P. R. Bhimireddy and A. Iqbal, "Distributed Fault-Tolerant Powertrain Configuration for Electric Vehicle Applications With Pole-Phase Modulation," *IEEE Trans. Ind. Electron.*, vol. 69, no. 8, pp. 7787–7796, Aug. 2022.

[10] Y. Wei, H. Li, Z. Zhou, and D. Chen, "Driving Path Tracking Strategy of Humanoid Robot Based on Improved Pure Tracking Algorithm," *IAENG International Journal of Applied Mathematics*, vol. 54, no. 2, pp286-297, 2024.

[11] L. Liu, K. Shi, X. Yuan, and Q. Li, "Multiple model-based fault-tolerant control system for distributed drive electric vehicle," *J Braz. Soc. Mech. Sci. Eng.*, vol. 41, no. 11, p. 531, Nov. 2019.

[12] Q. Li, H. Zhang, C. Gao, and S. Yan, "Research on failure classification and control strategy of four-wheel independent drive electric vehicle drive system," *J. Braz. Soc. Mech. Sci. Eng.*, vol. 43, no. 12, p. 550, Dec. 2021.

[13] X. Wang, P. Wu, S. Qu, and H. Wu, "Influence of Harmonic Components in Traction System on the Traction Motor of High-speed Train," *Engineering Letters*, vol. 32, no. 6, pp1163-1168, 2024.

[14] X. Zhang and V. Cocquempot, "Fault Tolerant Control for an Electric 4WD Vehicle's Path Tracking with Active Fault Diagnosis," *IFAC Proceedings Volumes*, vol. 47, no. 3, pp. 6728–6734, 2014.

[15] T. Chen, L. Chen, X. Xu, Y. Cai, H. Jiang, and X. Sun, "Passive fault-tolerant path following control of autonomous distributed drive electric vehicle considering steering system fault," *Mechanical Systems and Signal Processing*, vol. 123, pp. 298–315, May 2019.

[16] D. Zhang, G. Liu, H. Zhou, and W. Zhao, "Adaptive Sliding Mode Fault-Tolerant Coordination Control for Four-Wheel Independently Driven Electric Vehicles," *IEEE Transactions on Industrial Electronics*, vol. 65, no. 11, pp. 9090–9100, Nov. 2018.

[17] Y. Zhang, P. K. Wong, W. Li, Y. Cao, Z. Xie, and J. Zhao, "Fault diagnosis and fault tolerant control for distributed drive electric vehicles through integration of active front steering and direct yaw moment control," *Mechatronics*, vol. 97, p. 103116, Feb. 2024.

[18] H. Tang, Y. Chen, and A. Zhou, "Actuator Fault-Tolerant Control for Four-Wheel-Drive-by-Wire Electric Vehicle," *IEEE Transactions on Transportation Electrification*, vol. 8, no. 2, pp. 2361–2373, Jun. 2022.

[19] K. Ma, Z. Xie, P. K. Wong, W. Li, S. Chu, and J. Zhao, "Robust Takagi-Sugeno Fuzzy Fault Tolerant Control for Vehicle Lateral Dynamics Stabilization With Integrated Actuator Fault and Time Delay," *J. Dyn. Syst. Meas. Control-Trans. ASME*, vol. 144, no. 2, p. 021002, Feb. 2022.

[20] M. Zhao, H. Guo, L. Zhang, and X. Liu, "Driving Stability Control of Four-wheel Independent Steering Distributed Drive Electric Vehicle with Single Wheel Steering Failure," *Journal of Mechanical Engineering*, vol. 60, no. 10, pp. 507-522, 2024.

[21] J. Guo, J. Wang, Y. Luo, and K. Li, "Robust lateral control of autonomous four-wheel independent drive electric vehicles considering the roll effects and actuator faults," *Mech. Syst. Signal Proc.*, vol. 143, p. 106773, Sep. 2020.

[22] L. Zhang, W. Yu, Z. Wang, and X. Ding, "Fault tolerant control based on multi-methods switching for four-wheel-independently actuated electric vehicles," *Journal of Mechanical Engineering*, 2020, vol. 56, no. 16, pp. 227–239, 2020.

[23] Q. Li, J. Tang, B. Zhang, Y. Chen, and Y. Wang, "Research on Fault-Tolerant Control of Multi-Actuator for Distributed Drive Electric Vehicles," *Automotive Engineering*, 2023, vol. 45, no. 12, pp. 2251–2259, 2023.

[24] H. Zhou, F. Jia, Z. Liu, and H. Liu, "Fault diagnosis and fault-tolerant control method for in-wheel motor electric vehicles," *Journal of Mechanical Engineering*, vol. 55, no. 22, pp. 174–182, 2019.

[25] Y. Lu, J. Liang, W. Zhuang, G. Yin, J. Feng, and C. Zhou, "Four-wheel Independent Drive Vehicle Fault Tolerant Strategy using Stochastic Model Predictive Control with Model Parameter Uncertainties," *IEEE Trans. Veh. Technol.*, pp. 1–13, 2023.

[26] C. Li, G. Chen, C. Zong, and W. Liu, "Fault-Tolerant Control for 4WID/4WIS Electric Vehicle Based on EKF and SMC," *SAE Int. J. Passeng. Cars – Electron. Electr. Syst.*, vol. 9, no. 1, pp. 1–8, Sep. 2015.

[27] X. Peng, X. Xing, Q. Cui, and J. Huang, "Research on Driving Force Distribution Control Method of Distributed Electric Vehicles," *Automotive Engineering*, vol. 44, no. 07, pp. 1059–1068, 2022.

[28] J. Wang, R. Wang, H. Jing, and N. Chen, "Coordinated Active Steering and Four-Wheel Independently Driving/Braking Control with Control Allocation," *Asian Journal of Control*, vol. 18, no. 1, pp. 98–111, 2016.

[29] H. Yan, J. Fang, W. Ge, G. Wang, J. Chen, and C. Tan, "Modelling and Analysis of a Generalized Equivalent Magnetic Circuit Model for Moving Coil Electromagnetic Linear Actuators," *IAENG International Journal of Applied Mathematics*, vol. 54, no. 11, pp2299-2306, 2024.

[30] R. Wang and J. Wang, "Stability control of electric vehicles with four independently actuated wheels," in 2011 50th *IEEE Conference on Decision and Control and European Control Conference*, Dec. 2011, pp. 2511–2516.

[31] J. Hu, B. Zhang, H. Wang, L. Zhao, and P. Jiang, "Coordinated control and torque distribution of differential steering and anti-skid driving of distributed drive electric vehicle considering stability," *Proc. Inst. Mech. Eng. Part D-J. Automob. Eng.*, vol. 237, no. 12, pp. 2780–2796, Oct. 2023.

[32] E. Mousavinejad, Q.-L. Han, F. Yang, Y. Zhu, and L. Vlacic, "Integrated control of ground vehicles dynamics via advanced terminal sliding mode control," *Vehicle System Dynamics*, vol. 55, no. 2, pp. 268–294, Feb. 2017.

[33] A. Tavasoli, M. Naraghi, and H. Shakeri, "Optimized coordination of brakes and active steering for a 4WS passenger car," ISA Transactions, vol. 51, no. 5, pp. 573–583, Sep. 2012.

[34] P. Muthukumar, and M. Nirmala Devi, "Sliding Mode Control for Multi-scale Synchronization of Multi-scroll Fractional Order Chaotic Systems and Its Applications," *IAENG International Journal of Applied Mathematics*, vol. 54, no. 11, pp2343-2350, 2024.

[35] G. Pellegrino, A. Vagati, P. Guglielmi, and B. Boazzo, "Performance Comparison Between Surface-Mounted and Interior PM Motor Drives for Electric Vehicle Application," *IEEE Transactions on Industrial Electronics*, vol. 59, no. 2, pp. 803–811, Feb. 2012.

Zhigang Zhou is the professor of Henan University of Science and Technology. His research interests include dynamics and control of new energy vehicles, dynamics, and dynamic reliability of mechanical transmission systems.